Experimental and theoretical studies of electronic energy levels in InAs quantum dots grown on (001) and (113)B InP substrates

2002 J. Phys.: Condens. Matter 14 12301

(http://iopscience.iop.org/0953-8984/14/47/306)

INSTITUTE OF PHYSICS PUBLISHING JOURNAL OF PHYSICS: CONDENSED MATTER

J. Phys.: Condens. Matter **14** (2002) 12301–12309 PII: S0953-8984(02)37374-0

Experimental and theoretical studies of electronic energy levels in InAs quantum dots grown on (001) and (113)B InP substrates

P Miska, C Paranthoen, J Even, N Bertru, A Le Corre and O Dehaese

Laboratoire de Physique des Solides, INSA de Rennes, 20 Avenue des Buttes de Coesmes, CS 14315, F34043 Rennes Cedex, France

E-mail: jacky.even@insa-rennes.fr

Received 23 May 2002
Published 15 November 2002
Online at stacks.iop.org/JPhysCM/14/12301

Abstract

An experimental and theoretical comparative study of InAs quantum dots grown on (001) and (113)B InP substrates is performed. The difference between the optical transitions in the dots on the two substrates is attributed to strain effects. The influence of the first InP capping layer is also studied.

1. Introduction

Semiconductor quantum dots (QDs) produced by Stranski–Krastanov growth have attracted intensive research interest over the last few years because of their reduced dimensionality and the opportunity that they offer for the study of the confinement of electrons and holes [1, 2]. Moreover, QDs seem to be very promising for applications in many categories of semiconductor device. It has been demonstrated, for example, that QD lasers have superior characteristics: low threshold current densities, small chirp [3–7]. The growth of InAs QDs on InP substrates has been proposed, in order to achieve nanostructure-based devices emitting at the optical telecommunication wavelength (1.55 μm) [8–10]. Moreover, new growth methods have been developed for controlling the emission energy and reducing the photoluminescence (PL) linewidth [8]. Over the last few years, accurate theoretical models have been used to achieve a precise description of the electronic structure of QDs [11–13]. Among these models, the eight-band $\boldsymbol{k} \cdot \boldsymbol{p}$ Hamiltonian, together with the envelope function approximation, has been used more or less as a standard model, in the particular case of InAs QDs grown on GaAs substrates. However, in order to follow these approaches, a very good knowledge of the dot geometry, the material parameters, the chemical composition and the strain distribution is required [13, 14]. This has not been achieved yet for InAs QDs on InP substrate. Recently, a new growth procedure has been proposed, namely the double-cap (DC) process, which has proved to be efficient for controlling the dot height and reducing drastically the height dispersion [8], but a precise experimental description of all the dot parameters is still lacking.

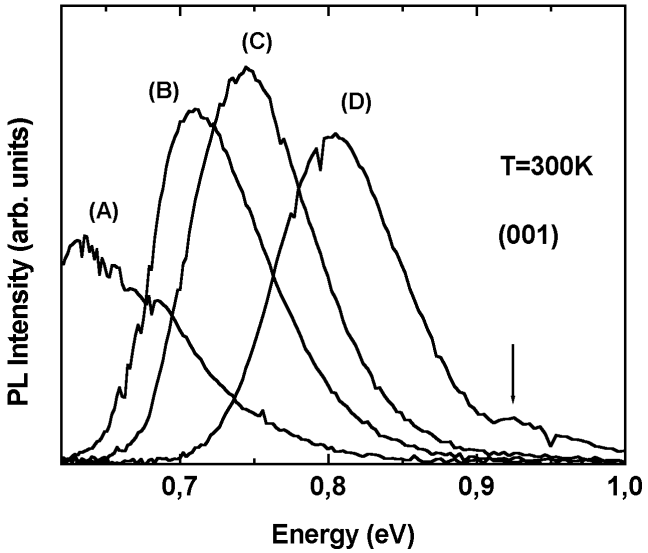

Figure 1. PL spectra measured at room temperature from samples grown with various thicknesses of the first InP cap layer. The substrate orientation is (001). Sample A is a reference sample without an InP capping layer. Samples D, C, B correspond to first-InP-cap-layer thickness equal to respectively 2, 3 and 4 nm. The WL luminescence is indicated by an arrow.

In this work we have performed a first experimental and theoretical comparative study of InAs QDs grown following the DC procedure [8] either on (001) or on (113)B InP substrate. A simplified theoretical model is used, taking into account strain and surface orientation.

2. Experimental study

The experimental details of the sample growth have been presented in earlier papers [8, 15, 16]. The InAs QDs were grown at 480 °C on an InP lattice-matched $Ga_{0.2}In_{0.8}As_{0.435}P_{0.565}$ ($Q_{1.18}$) buffer layer during the same growth run on (001) or (113)B InP substrates, using a gas source molecular beam epitaxy system. Firstly, the QDs are formed by the deposition of 2.1 monolayers of InAs. Then, the DC growth procedure is carried out. A first thin InP layer (the first cap layer) is deposited to completely cover the smallest dots, leaving the top of the biggest dots free. Then an annealing under P_2 flux during the growth turns the non-covered InAs part of the biggest dots into an InAsP alloy. The main effect is that the height of the biggest island is strongly reduced. Finally, the growth of a $Q_{1.18}$ layer is carried out.

Figures 1 and 2 show PL spectra recorded on QD samples grown on (001) and (113)B surfaces respectively. In both cases, sample A is a reference sample without an InP capping layer and growth interruption, i.e. as-grown QDs. Samples B, C, D correspond to DC QDs, with a first-InP-cap-layer thickness equal to 40, 30 and 20 Å respectively. First, comparison of the spectra A of the as-grown QDs samples enable us to propose several characteristics of the QDs grown with the two different substrate orientations. The (001) QDs are characterized by a very broad FWHM (full width at half-maximum) of the PL peak (>100 meV) and a low optical emission energy (<0.7 eV), in comparison with those grown on the (113)B substrate (71 meV and 0.7 eV respectively). This indicates a narrower height dispersion of the QDs grown on InP (113)B substrates. Indeed, the height histogram of the uncapped InAs QDs grown on the (001) InP substrate reveals that the height distribution is very large when compared to that for the (113)B substrate [15]. The smaller QD height on the (113)B substrate may also explain

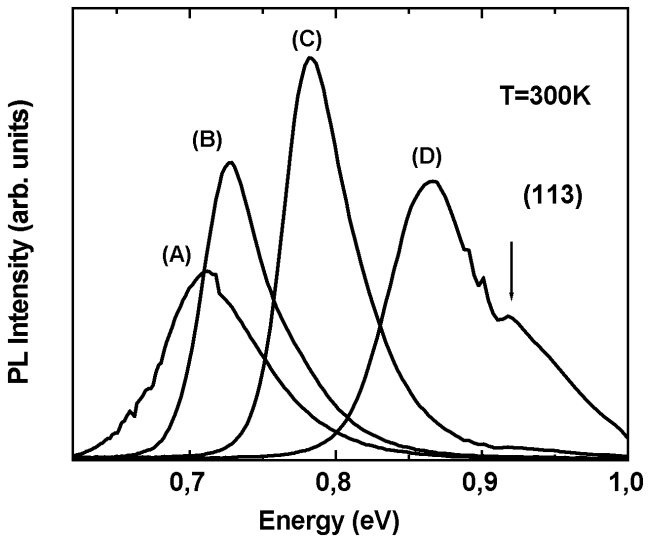

Figure 2. PL spectra measured at room temperature from samples grown with various thicknesses of the first InP cap layer. The substrate orientation is (113)B. Sample A is a reference sample without an InP capping layer. Samples D, C, B correspond to InP cap layer thickness equal to respectively 2, 3 and 4 nm. The WL luminescence is indicated by an arrow.

the higher optical emission energy. The capped QDs grown on (001) and (113)B substrates have been estimated to be 70 and 50 Å high and 450 and 350 Å wide [15] respectively. On applying the DC procedure (spectra B, C, D), one can see a clear blue-shift of the QD emission of about 180 meV for the (113)B QDs. This clearly indicates that the quantum confinement increases with decreasing QD height, which means that the dot heights are effectively reduced as expected. For QDs grown on (113)B substrate, it has been shown that the PL linewidth changes from 70 meV for the reference sample to 50 meV for the sample with a first-cap-layer thickness equal to 30 Å, despite the detrimental effect of a higher confinement [8]. The same phenomenon is observed for QDs grown on (001) substrate (figure 1). For the same first-cap-layer thickness of 30 Å, the PL linewidth is then equal to 50 meV on the (113)B InP surface (figure 2) and 95 meV on the (001) InP surface (figure 1). This effect is probably related to the larger height distribution measured for uncapped QDs grown on (001) InP surfaces [15]. Arrows in figures 1 and 2 indicate that for sample D, luminescence from the wetting layer (WL) is observed. In both cases, the WL luminescence peak is located at about 0.92 eV. The WL luminescence is enhanced for the (113)B sample. This is probably due to a stronger QD–WL electronic coupling in that case. The QD luminescence is observed at 0.805 eV for the (001) sample and 0.875 eV for the (113)B sample, closer to the WL luminescence energy.

3. Theoretical study

We present now a first attempt to study theoretically two effects which are important for the electronic and optical properties of InAs grown on InP substrate by the DC procedure. The first effect is due to the orientation of the InP substrate. The second effect is the quantum confinement related to the thickness of the first cap layer. When considering both effects, we must point out that a precise experimental description of the dot parameters (shape, strain, composition, ...), as in the case of InAs/GaAs [14], is lacking. Therefore we have decided to use simplified models. We model the deformation of capped QDs on the (001)-or (113)B-oriented substrate surfaces assuming that they are equivalent to epitaxial layers with a coherent

interface [17, 18]. This approximation may be justified: first, the QDs height/width ratio is very small ($\sim 1/10$) and, second, the QDs grown by the DC procedure are truncated with a flattened upper surface [8]. For the reference system of the cubic lattice, the deformation tensor for the InAs layer on the (001) and on the (113)B InP substrates are calculated:

$$e_{ij} = \begin{bmatrix} -0.031 & 0 & 0 \\ 0 & -0.031 & 0 \\ 0 & 0 & 0.034 \end{bmatrix} \quad (001) \qquad e_{ij} = \begin{bmatrix} -0.030 & 0.001 & 0.011 \\ 0.001 & -0.030 & 0.011 \\ 0.011 & 0.011 & 0.026 \end{bmatrix} \quad (113)\text{B}.$$

For the (001)-oriented InP surface, the strain tensor is due to a biaxial compression leading to tetragonal deformation of the InAs lattice. For the (113)B-oriented InP surface, shear strains appear. Our approximation corresponds to homogeneous deformations inside the QD. Some authors [19] have performed accurate strain calculations for InAs/GaAs QDs of various shapes. For flat and wide QDs, they found that the strain components do not extend through the QD and that the constant-strain approximation is quite reasonable. The same conclusion is drawn for InAs/InP(001) QDs using an atomistic valence force-field description [20]. This is consistent with Raman scattering experimental results for InAs/InP(001) QDs [21].

In [22], the authors developed an electronic model for InAs/GaAs QDs. A one-particle Hamiltonian is defined for QDs with cylindrical symmetry. A one-band effective mass approximation is used both for the conduction band (CB) and for the valence band (VB). This approach yields interesting results if the mechanical strain is taken into account to renormalize the energy gaps and effective VB and CB masses [23, 24]. But in the compressive case of quantum wells, two other effects are predicted: the effective CB mass becomes anisotropic and the light-hole (LH) band shifts below the heavy-hole (HH) band [23]. A one-band effective mass approximation with renormalized band gaps and effective VB and CB masses is not able to reproduce the effect of strong band mixing. Non-parabolic dispersions of the HH and LH bands may be associated with HH–LH band mixing. It has previously been shown [19], however, that for flat and wide QDs, the HH and LH potentials are well separated. For that reason, we consider the HH band alone with a renormalized potential and renormalized effective masses only. In our model the CB band is also decoupled from the other bands but with a renormalized potential and renormalized effective masses. It is important to notice that for InAs/InP QDs the influence of strains is less important than for InAs/GaAs QDs, because the lattice mismatch is only equal to about 3.1% in the former case whereas it is equal to 7.2% in the latter case.

The strained $8 \times 8\boldsymbol{k} \cdot \boldsymbol{p}$ Hamiltonian [25] for bulk strained InAs has been used to calculate the 3D dispersion curves and effective masses in the reference system of the cubic lattice (crystallographic axes) and in the reference system of the epitaxial layer for the (001) surface and for the (113)B surface. In this last case, the basis vectors in the reference system of the epitaxial layer are $[3, 3, \bar{2}]$, $[\bar{1}, 1, 0]$ and [113]. Band structure parameters for InAs have been taken from [26]. Figure 3 shows the dispersion curves for bulk InAs strained on the (113)B surface calculated at $T = 0$ K. The HH band is decoupled from the LH band. The CB band and HH band dispersion curves along the [113] growth axis are different from the ones along the $[3, 3, \bar{2}]$ and $[\bar{1}, 1, 0]$ axes. There is a strong anisotropy between the in-plane (growth plane) masses and the out-of-plane mass. There is also a small anisotropy in the growth plane between the $[3, 3, \bar{2}]$ and $[\bar{1}, 1, 0]$ directions. This anisotropy is neglected in our calculations and a mean value is considered for the CB and HH in-plane masses. An important result is that the gap between CB and HH bands increases at low temperature (2 K) from 0.418 eV for unstrained InAs to 0.536 eV for bulk InAs strained on the (113)B InP surface. For bulk InAs strained on the (001) InP surface, the gap is equal to 0.494 eV. The effect of substrate orientation is then estimated to be 42 meV for the gap. The CB and HH parabolic band structure parameters are

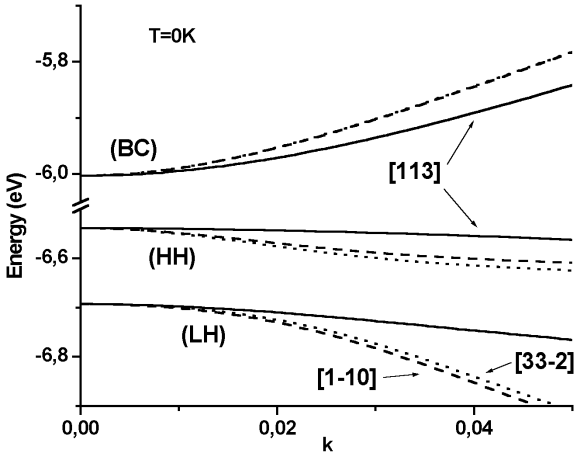

Figure 3. Electronic energy dispersion curves calculated from a 8 × 8 bulk strained Hamiltonian in the case of (113)B InP substrate. The [33$\bar{2}$], [1$\bar{1}$0] and [113] directions are indicated. BC, HH and LH correspond respectively to the conduction, HH and LH bands.

Table 1. The CB and HH parabolic band structure parameters and confinement potentials with respect to CB and VB bands of the $Q_{1.18}$ buffer layer.

	(001) surface	(113)B surface
E_{gap} (meV)	494	536
m_{HH}^{in}	0.032	0.034
m_{HH}^{out}	0.341	0.336
m_{CB}^{in}	0.025	0.027
m_{CB}^{out}	0.044	0.045
$V_{conf\,HH}$ (meV)	364	356
$V_{conf\,CB}$ (meV)	391	356

reported in table 1 together with the CB and HH confinement potentials with respect to CB and VB bands of the $Q_{1.18}$ buffer layer.

A simple geometry of the QDs is considered in the simulation. The reference capped QDs are represented by half of an ellipsoid. On the (001) substrate, the height is 70 Å and the diameter 450 Å [15]. On the (113)B substrate, the height is 50 Å and the diameter 350 Å [8]. The effect of the first cap layer for DC QDs is simulated by truncating the top of the ellipsoid above the first-cap-layer thickness (40, 30 or 20 Å) (figure 4(a)). There is a cylindrical symmetry because the QD geometry is unchanged by applying any rotation around the growth axis ($C_{\infty v}$ symmetry group). The $\boldsymbol{k}\cdot\boldsymbol{p}$ Hamiltonian representation of the Bloch functions is compatible with a cylindrical representation used in [22]. The one-particle Hamiltonian can be written either for the HH or for the electron [22]:

$$H = H^z + H^{r,\theta} + V(r,z) \tag{1}$$

with

$$\begin{aligned} H^z &= -\frac{\hbar^2}{2}\frac{\partial}{\partial z}\frac{1}{m^z_{(r,z)}}\frac{\partial}{\partial z} \\ H^{r,\theta} &= -\frac{\hbar^2}{2}\left[\frac{1}{r}\frac{\partial}{\partial r}\frac{r}{m^r_{(r,z)}}\frac{\partial}{\partial r} + \frac{1}{m^r_{(r,z)}}\frac{\partial^2}{r^2\,\partial\theta^2}\right]. \end{aligned} \tag{2}$$

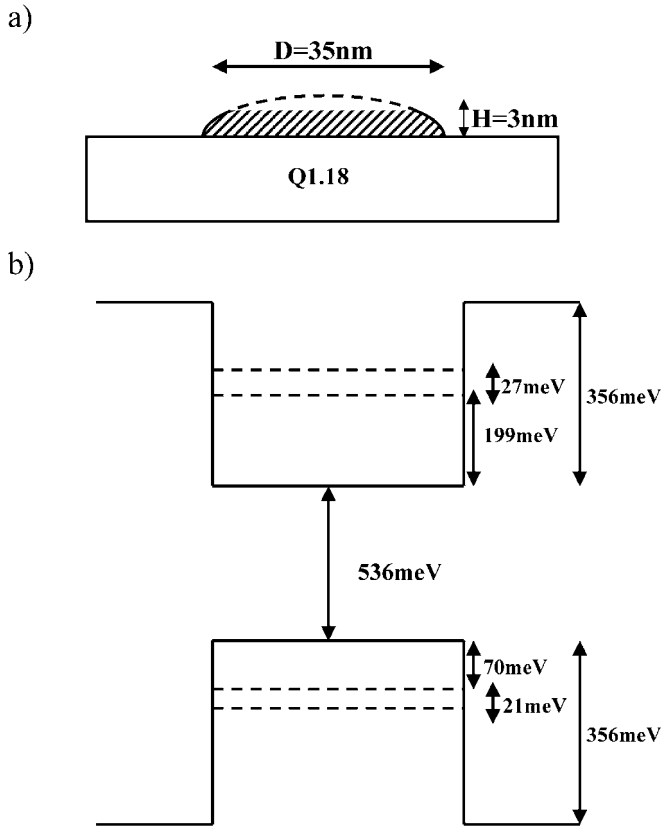

Figure 4. (a) The shape of the QD considered in the calculation corresponds to a truncated ellipsoid. H is the height of the QD and D is the diameter of the ellipsoid. (b) Electronic energy levels calculated at $T = 0$ K for a $H = 3$ nm QD grown on the (113)B surface.

Due to the cylindrical symmetry, the confinement potential $V(r, z)$ is not separable and couples the motions along z and in the (r, θ) plane. The variables r and z are also coupled by the non-separable dependence of these effective masses along z and r. Taking into account the commutation of H and $\partial/\partial\theta$, the eigenfunctions of the Schrödinger equation can be calculated as $\Psi(r, \theta, z) = \varphi(r, z)\mathrm{e}^{\mathrm{i}n\theta}$ where n is the angular momentum and the new expression for $H^{r,\theta}$ is

$$H^{r,\theta} = -\frac{h^2}{2}\left[\frac{1}{r}\frac{\partial}{\partial r}\frac{r}{m^r_{(r,z)}}\frac{\partial}{\partial r} - \frac{n^2}{m^r_{(r,z)}r^2}\right]. \tag{3}$$

In [22], the authors study cones such as InAs/GaAs QDs. The solution of the one-particle Hamiltonian was decomposed in the finite basis of symmetry-adapted orthonormalized functions formed by the products of Bessel functions of integer order n (angular momentum) and sine functions of z. We applied a 2D finite-difference method to the one-particle Hamiltonian with a variable step along the z-axis in order to achieve a good precision for numerical computations. For simple cylindrical or conical shapes, we checked that the finite-difference method yield the same results as the method of [22]. The energy levels may be labelled according to the n-value: for S states, $n = 0$; for P states, $n = 1$; and for D states, $n = 2$.

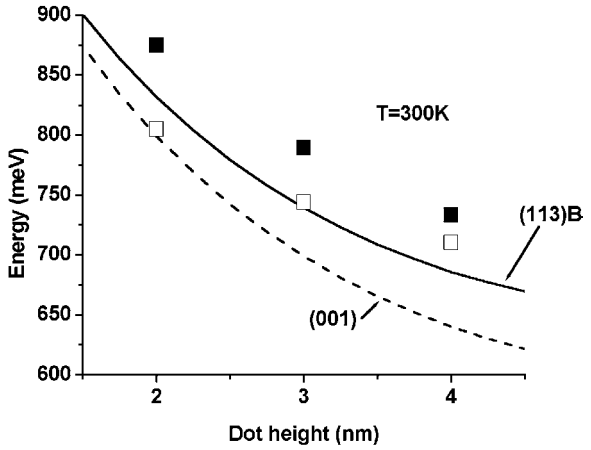

Figure 5. Evolution of the gap (fundamental 1s–1s optical transition energy) as a function of dot height. Theoretically calculated transition energies are represented by a continuous curve ((113)B surface) or a dashed curve ((001) surface). Experimental points are indicated in the same figure assuming that the InP capping layer thickness is equal to the dot height. The closed and open squares correspond respectively to the QDs on the (113)B and (001) surfaces.

Figure 4(b) shows the electronic spectrum for an InAs DC QD grown on a (113)B InP substrate with $Q_{1.18}$ buffer layers. The thickness of the first InP cap layer is equal to 30 Å. The fundamental optical transition corresponds to the 1S–1S CB–HH electronic transition. The first optical transition between excited 1P states is predicted to be 48 meV above the 1S–1S fundamental transition. This is smaller than comparative values for InAs/GaAs QDs. Further experimental studies must be performed in order to check this result.

Figure 5 shows the evolution of the 1S–1S transition energy as a function of the dot height. Experimental points (assuming the dot height to be the thickness of the first cap layer) and theoretical curves are reported for both the (001) and (113)B InP substrates. Experimental measurements and theoretical calculations show that the gap between BC and HH bands is larger for the (113)B InP surface. This effect may be mainly due to the increase of the strained bulk InAs gap. These curves also indicate that there is not a linear relation between the transition energy and the dot height. The experimental transition energy for the dot height corresponds to a smaller effective thickness in the theoretical calculations. The differences between the InP capping layer thicknesses and effective calculated heights are equal to about 0.5 nm. This may be attributed to As/P exchange, which tends to reduce the height of the QD [8]. An important difference between InAs/InP and InAs/GaAs lies in the fact that in the former case the III element is common. As/P exchanges play an important role during the growth of InAs/InP QDs. Indeed, the growth interruption performed under phosphorus flux and the growth of a $Q_{1.18}$ buffer layer do not correspond to the simple truncation of the QD [15]. It is known that these two processes lead to further reductions of the height for all the QDs. The height reduction is certainly less effective for small DC QDs than for large QDs. This interpretation is consistent with the fact that the height distribution is narrowed but also shifted (figures 1 and 2). It may also explain why the effective thickness in the theoretical calculations is smaller than the capping layer thickness.

In figure 5, we may also notice that the variation between the calculated transition energy and the dot height is parallel to the variation between the experimental transition energy and the capping layer thickness only for the (113)B InP substrate. For the (001) InP substrate, the

difference between the two curves decreases with the QD height. A possible explanation for this observation is that growth interruption under phosphorus used previously for QD growth on (113)B InP substrate [8] has a different effect for QDs grown on (001) InP substrate. The protection due to the capping layer could be different in that case, leading to a larger effective thickness for smaller capping layer thickness. A second possible explanation is that the lateral quantum confinement is less important and different for QDs grown on (001) InP substrate. Indeed it is known that the 2D–0D transition during the growth is difficult on (001) InP substrate [21] due to the low lattice mismatch between InAs and InP. This is one of the reasons that the (113)B InP substrate has been chosen [8]. QDs, quantum wires or even separated quantum wells are formed on (001) InP substrate, depending on the growth conditions [27]. Weak changes of the growth conditions lead to large changes of the nanostructure lateral morphology. A recent magnetoluminescence study [28] shows that the high-energy optical transitions sometimes observed for InAs QDs grown on (001) InP substrate are different to the ones for InAs QDs grown on (001) GaAs substrate. These latter may be clearly attributed to p or d electronic states.

We finally add a comment on the internal piezoelectric field effect in InAs/InP QDs. The presence of piezoelectric effects in strained layer heterostructures is well known for high-index substrates and is related to off-diagonal homogeneous strains [29–31]. There is a lack of information on the role of piezoelectric effects in the optical properties of QDs [32, 33]. In addition to the above-described off-diagonal homogeneous strains, further ones related to the QD shape may appear. We believe, however, that, as pointed out by the authors of [33], for flat QDs piezoelectric effects associated with off-diagonal inhomogeneous strains are not important. Off-diagonal homogeneous strains may however induce a piezoelectric field and a permanent polarization for QDs grown on (113) InP substrate. It is possible to evaluate the internal piezoelectric field on the basis of our uniformly strained 2D InAs slab model [29, 32]. The permanent polarization calculated in the reference system of the epitaxial layer is then equal to $(1.24, 0, 0.69) \times 10^{-3}$ C m^{-2}. There is no polarization along the $[\bar{1}, 1, 0]$ direction for symmetry reasons. The internal piezoelectric field is along the [1, 1, 3] direction and is equal to 51 kV cm^{-1}. This value is much smaller than the one calculated for InAs QDs grown on (113) GaAs substrate [32]. This is due to the smaller lattice mismatch between InAs and InP. Experimental determination by the method proposed in [33] is possible. Such work is in progress in our laboratory on p–i–n devices [34]. However, the quantum-confined Stark shift (QCSS) is not expected to be important in our case. In [33], for an internal piezoelectric field equal to 170 kV cm^{-1}, the QCSS is found experimentally to be on the order of 2–3 meV. The QCSS is a quadratic effect; thus we do not expect a large QCSS for a value of 51 kV cm^{-1}. The difference between quantum wells and QDs can be understood on the basis of the QCSS formula for quantum wells with an infinite confinement potential [26, 31]. This formula contains an L^4-dependence on the quantum well thickness. As a first approximation, one may consider our flat QDs to be about three times thinner than conventional quantum wells and may expect the QCSS to be very small.

4. Conclusions

We have performed an experimental and theoretical comparative study of the electronic energy levels and optical transitions in InAs QDs grown on (001) and (113)B InP substrates. The differences between the optical transitions in the QDs on the two substrates are mainly due to strain effects. The variation of the optical transition energy as a function of the first-cap-layer thickness was measured. It was compared to the calculated optical transition energy as a function of the dot height. The theoretical calculations predict that the difference between the

1s–1s and 1p–1p optical transitions is smaller than in the InAs/GaAs system. The theoretical model is a first attempt to calculate electronic properties of InAs/InP QDs. It may be improved by going beyond the cylindrical approximation and by using the 8×8 strained Hamiltonian for the envelope functions. Further experimental work should also be performed to get a better description of the InAs/InP QDs geometry, composition and strains.

References

[1] Sugawara M (ed) 1999 *Self-Assembled InGaAs/GaAs Quantum Dots (Semiconductors and Semimetals vol 60)* (San Diego, CA: Academic)

[2] Bimberg D, Grundmann M and Ledentsov N N 1998 *Quantum Dot Heterostructures* (Chichester: Wiley)

[3] Grundmann M 2000 *Physica* E **5** 167

[4] Grundmann M 2000 *Appl. Phys. Lett.* **77** 1428

[5] Bimberg D and Ledentsov N N 2000 *Physics and Simulation of Optoelectronic Devices VIII (Proc. SPIE vol 3944)* ed R Binder, P Blood and M Osinski (Bellingham, WA: SPIE Optical Engineering Press) p 790

[6] Newell T 1999 *IEE Photon. Technol. Lett.* **11** 1527

[7] Gerard J M, Lemaître A, Legrand B, Ponchet A, Gayral D and Thierry-Mieg V 1999 *J. Cryst. Growth* **201** 1109

[8] Paranthoen C, Bertru N, Dehaese O, Le Corre A, Loualiche S, Lambert B and Patriarche G 2000 *Appl. Phys. Lett.* **78** 1751

[9] Saito H, Nishi K and Sugou S 2001 *Appl. Phys. Lett.* **78** 267

[10] Paranthoen C, Bertru N, Lambert B, Dehaese O, Le Corre A, Even J, Loualiche S, Lissilour F, Moreau G and Simon J 2002 *Semicond. Sci. Technol.* **17** L5

[11] Wang L W, Williamson A J, Zunger A, Jiang H and Singh J 2000 *Appl. Phys. Lett.* **76** 339

[12] Stier O, Grundmann M and Bimberg D 1999 *Phys. Rev.* B **59** 5688

[13] Pryor C 1999 *Phys. Rev.* B **60** 2869

[14] Shumway J, Williamson A, Zunger A, Passaseo A, DeGiorgi M, Cingolani R, Catalano M and Crozier P 2001 *Phys. Rev.* B **64** 125302

[15] Fréchengues S, Drouot V, Bertru N, Lambert B, Loualiche S and Le Corre A 1999 *J. Cryst. Growth* **201** 1180

[16] Fréchengues S, Drouot V, Paranthoen C, Dehaese O, Loualiche S, Le Corre A and Lambert B 2000 *J. Cryst. Growth* **209** 661

[17] Yang K, Anan T and Schowalter L 1994 *Appl. Phys. Lett.* **65** 2789

[18] Lacombe D, Ponchet A, Fréchengues S, Drouot V, Bertru N, Lambert B and Le Corre A 1999 *Appl. Phys. Lett.* **74** 1680

[19] Cusack M, Briddon P and Jaros M 1997 *Phys. Rev.* B **56** 4047

[20] Groenen J, Priester C and Carles R 1999 *Phys. Rev.* B **60** 16013

[21] Ponchet A, Le Corre A, L'Haridon H, Lambert B, Salaun S, Groenen G and Carles R 1996 *Solid State Electron.* **40** 615

[22] Marzin J Y and Bastard G 1994 *Solid State Commun.* **92** 437

[23] Chao C and Chuang S 1992 *Phys. Rev.* B **46** 4110

[24] Fonseca L, Jimenez J, Leburton J and Martin R 1998 *Phys. Rev.* B **57** 4017

[25] Bahder T 1990 *Phys. Rev.* B **41** 11992

[26] Chuang S 1995 *Physics of Optoelectronic Devices* ed J W Goodman (New York: Wiley)

[27] Paranthoen C, Bertru N, Dehaese O, Le Corre A and Folliot H 2002 *Crystal Growth in Thin Solid Films: Control of Epitaxy* ed M G Viry and A Perrin (Trivandrum: Transworld Research Network Publisher) at press

[28] Raymond S, Studenikin S, Ciorga M, Piono-Ladrière M, Zawadzki P, Korkusinski M, Hawrylak P, Gauthier V, Poole P J and Sachradja A 2002 *Proc. 26th Int. Conf. on the Physics of Semiconductors (Edinburgh, UK)* at press

[29] Smith D L and Mailhiot C 1990 *Rev. Mod. Phys.* **62** 173

[30] Smith D L 1997 *Microelectron. J.* **28** 707

[31] Tomasini P, Arai K, Lu F, Zhu Z Q, Sekiguchi T, Suezawa M, Yao T, Shen M Y, Goto T, Yasuda T and Segawa Y 1998 *J. Appl. Phys.* **83** 4272

[32] Sanguinetti S, Gurioli M, Grilli E, Guzzi M and Henini M 2000 *Appl. Phys. Lett.* **77** 1982

[33] Patane A, Levin A, Polimeni A, Schindler F, Main P C, Eaves L and Henini M 2000 *Appl. Phys. Lett.* **77** 2979

[34] Miska P, Sakri A, Even J, Lemoine D, Dehaese O, Folliot H, Labbé C, Senes M and Marie X 2002 *Proc. 26th Int. Conf. on the Physics of Semiconductors (Edinburgh, UK)* at press